

Investigation of the Structure, Elemental and Phase Composition of Coatings on the Basis of Oxynitride Titanium Deposited by Reactive Magnetron Sputtering

N. N. Nikitenkov^a, E. S. Kiselyova^a, M. E. Konischev^a, V. S. Sypchenko^a, A. N. Nikitenkov^a,
V. F. Pichugin^a, I. A. Shylepov^a, and M. Eppe^b

^aNational Research Tomsk Polytechnic University, Tomsk, 634050 Russia

^bInstitut für Anorganische Chemie Duisburg-Essen, Essen, 45117 Germany

e-mail: Nikitenkov@tpu.ru, Felistag@mail.ru

Received June 23, 2014

Abstract—The structure, morphology and properties of titanium-oxynitride coatings deposited by pulsed reactive magnetron sputtering were investigated. The methods of X-ray diffractometry, Raman spectroscopy, secondary ion mass-spectrometry and scanning electron microscopy are used. It is established that the structure, and the elemental and phase composition of coatings depend on the size of the ratio of oxygen/nitrogen in the composition of the reactive gas, and also on the magnitude of the negative bias applied to the substrate. The increase in the fraction of nitrogen leads to a reduction in the speed of sputtering, to a reduction in the contact angle of wetting, an increase in hardness and a reduction in Young's modulus when a negative offset was used.

DOI: 10.1134/S1027451014060391

INTRODUCTION

Interest in oxynitride coatings of titanium is due to the fact that the variation in the oxygen/nitrogen ratio in their composition leads to the appearance of unexpected and promising properties for coatings [1–5]. Different chemical and physical methods are used for deposition of the films, which make it possible to obtain coatings with different O/N values. Reactive magnetron sputtering makes it possible to change the O/N ratio in the composition of the coating flexibly and in a wide range, and to obtain a sample with deterministic structure and properties [2]. In addition, due to high biological compatibility, it is quite promising to use the oxynitride coating of titanium in medicine. For example, coatings on the basis of titanium oxynitrides can improve the anti-thrombosis properties of cardiovascular implants [6].

In this work we present the results of studying the properties, structure and morphology of titanium-oxynitride coatings deposited by the method of pulse reactive magnetron sputtering. The coatings are saturated with hydrogen, and their ability to accumulate and store it is studied, since structures of such type can serve as effective accumulators of hydrogen, which is topical in hydrogen energetics [3]. In addition, the presence of hydrogen in the coating is apparently capable of affecting its biological compatibility.

MATERIALS AND METHODS OF STUDY

In order to deposit oxynitride coatings, we designed and manufactured a reactive magnetron sputtering installation with a disc sputtering system designed in the form of a monoblock [3, 7]. Coating deposition is performed in the mode of ion bombardment, upon which the workstation is supplied with negative voltage in-phase with the power-supply pulse of the magnetron. The system of pulse negative bias makes it possible to supply voltage to the substrate creating the necessary conditions for the acceleration of low-energy ions. A mixture of oxygen (O₂) and nitrogen (N₂) was used as the plasma-forming gas. The substrates were samples of stainless steel of 12Kh18N10T grade and silicon (Si) plates. The material of the cathode is Ti, the working pressure in the chamber is 10⁻¹ Pa, the power and current values are 1 kW and 3 A, respectively. The temperature of the sample surface during deposition was 380 K, the velocity of the working-gas input was 5 mL/min, the bias voltage $U_{\text{bias}} = -60$ V, -100 V, the ratio of the partial gas pressure $p(\text{O}_2)/p(\text{N}_2) = 1/1; 1/2; 1/3; 1/4; 1/5$. The repetition pulse rate is 60 kHz, and the filling factor is 85%. Ellipsometric measurements of the coating thickness were performed on an Ellips-1891 SAG spectral complex at a fixed incidence angle of light of 70° in the wavelength range $\lambda = 250$ –1000 nm. Experimental optical “air–TiO₂–substrate”; “air–TiON–substrate” models were designed. The structure of the coating surface and its elemental com-

Table 1. Modes of the formation of coating samples: U_{bias} is the electrical bias; O/N is the value of the ratio oxygen/nitrogen in the composition of the reaction gas; n is the refraction index

Sample no.	Composition	U_{bias} , V	O/N	Thickness, nm	n	Sample no.	Composition	U_{bias} , V	O/N	Thickness, nm	n
0	TiO ₂	—	—			2	TiON	—	1/2	218 ± 13	
0 ₁	TiO ₂	60	—	174	2.44	3	TiON	—	1/3	167 ± 9	
0 ₂	TiO ₂	100	—	152	2.60	3 ₁	TiON	60	1/3	199	2.20
1	TiON	—	1	192 ± 8		3 ₂	TiON	100	1/3	210	2.25
1 ₁	TiON	60	1	180	2.30	4	TiON	—	1/4	116 ± 5	
1 ₂	TiON	100	1	185	2.46	5	TiON	—	1/5	218 ± 6	

position were studied using an ESEM Quanta 400 FEG scanning electron microscope (SEM) from FEI with a built-in EDX analyzer (Genesis 4000, S-UTW-Si(Li)). The method of energy dispersive X-ray analysis provided data about the elemental composition of the coatings. To study the structure and phase composition of the coating, we used an X-ray diffractometer (XRD, D8 Advance, Bruker, Germany), shooting in grazing geometry (CuK_α radiation $\lambda = 0.154$ nm, voltage 40 kV, current 40 mA). The structure of the deposited films was studied by the method of Raman spectroscopy. The combined-scattering spectra were obtained using a Centaur U HR complex, the spectrometer provided a resolution of 0/01 nm obtained through the use of a monochromator with double dispersion. A single-mode laser with a wavelength of 532.8 nm, power of 50 mW, and diameter of the beam focused on the surface of 10 μm was used as the radiation source. The film composition over depth using a Raman spectrometer was studied by successive scanning of the characteristic points on the slope of the crater formed in samples as a result of their investigation by the method of secondary ion mass-spectrometry [3]. The hardness and Young's modulus of the coatings were measured using a nano hardness tester (Nano Hardness Tester). The contact wetting angle θ and the surface energy σ were measured using a Kruss Easy Drop instrument [8]. Hydrogen saturation was implemented by the Sieverts method at a hydrogen pressure of 5 atm and a sample temperature of 500°C for 2 h. The atomic and molecular composition of the surface layers of the sample was studied by the method of secondary ion mass-spectrometry [3] using an MS-7201M instrument. The modes of coating formation are given in Table 1.

RESULTS AND DISCUSSION

Studies of the morphology of the coatings by the method of scanning electron microscopy show that they have a fine-grained structure. The average grain size depends on the composition of the reaction gas and for different samples is the following: no. 1—158 nm; no. 2—85 nm; no. 3—85 nm; no. 4—305 nm; no. 5—101 nm. It can be seen in Figs. 1a and 1b that

the fraction of the grain boundaries in the film is high. The structure of the obtained coatings can be interpreted within the band diagram [8]. The coating on the basis of TiO₂ has a columnar structure (Fig. 1c). The melting temperature of TiO₂ is 2113 K, the ratio of the substrate temperature to the melting temperature $T_{\text{subst}}/T_{\text{melt}} = 0.18$. According to the Thornton band diagram [8], the microstructure observed in Fig. 1c refers to band 1 of the diagram. The films consist of columnar grains with rather dense packing. Diffusion processes are weakly developed in this band because of the low mobility of atoms. The presence of nitrogen in the composition of the reaction gas leads to a decrease in the size of structural elements of the coating (Fig. 1d).

The measurements performed by the method of energy dispersive X-ray spectroscopy make it possible to estimate the ratio of the concentrations of chemical elements in the coating. It was found that all elements present in the plasma magnetron discharge are present in the film: titanium, oxygen, and nitrogen. The ratio of the concentrations O/N in the coating depends on the composition of the reaction gas and increases with an increase in nitrogen. For sample no. 1 at $p(\text{O}_2)/p(\text{N}_2) = 1$ the ratio O/N = 4.7; for sample no. 3 at $p(\text{O}_2)/p(\text{N}_2) = 1/3$ the ratio O/N = 3.8.

The distribution of the yield of secondary ions of the main elements during sputtering of the surface of the film–substrate system obtained by the method of secondary ion mass-spectrometry shows that they are distributed uniformly over coating depth. Figure 2 shows the distribution of the yield of secondary ions of the main elements during sputtering of the surface of film–sample system no. 1₂ TiON, and Fig. 3 shows data for sample no. 1₂ TiON saturated with hydrogen. It is seen that hydrogen saturation leads to the diffusion of Cr⁺ ions from the substrate into the film through the film–substrate interface to a distance of 80 nm. The X-ray analysis data show that TiO₂ with the anatase structure is present in the film. Figure 4 shows the Raman scattering spectra for eight points on sample surface no. 1₂ TiON (in total for each sample the spectra were measured at 30 points uniformly distributed on the surface). We note that the spectra

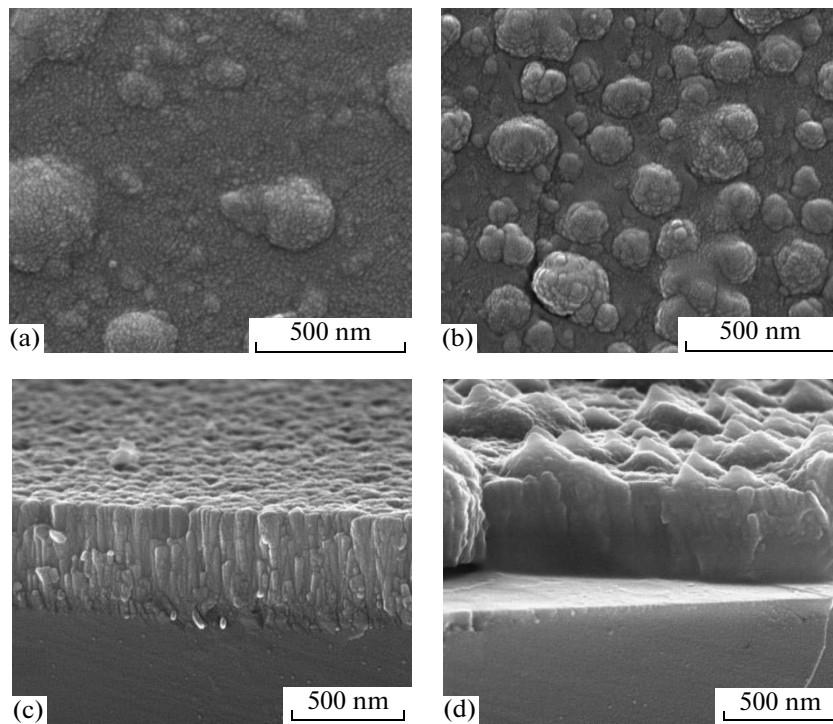


Fig. 1. SEM images of coatings: TiO₂ (a); Ti–O–N, no. 4 (b); TiO₂, transverse cross section (c); Ti–O–N, no. 4, transverse cross section (d).

strongly differ from point to point and not always are all peaks characteristic for anatase revealed at room temperature [3, 9]: E_g1 (139.2 cm^{-1}), E_g2 (190 cm^{-1}), B_{1g} (397.2 cm^{-1}), $(A_{1g} + B_{1g})$ (516 cm^{-1}), E_g3 (641 cm^{-1}). The modes E_g1 , E_g2 and B_{1g} show the shift to the long-wavelength region. These data indicate that during the process of deposition in the “displacement” mode anatase is the dominant crystalline phase in the coat-

ing, which is explained by the high chemical activity of oxygen present in this sample in a larger amount than nitrogen in comparison with other samples. Such a result is apparently associated with an increase in the nitrogen concentration in the mixture of reaction gases and with the fact that nitrogen appears in the composition of the coatings during the application of electrical bias. In the given sample nitrogen is present

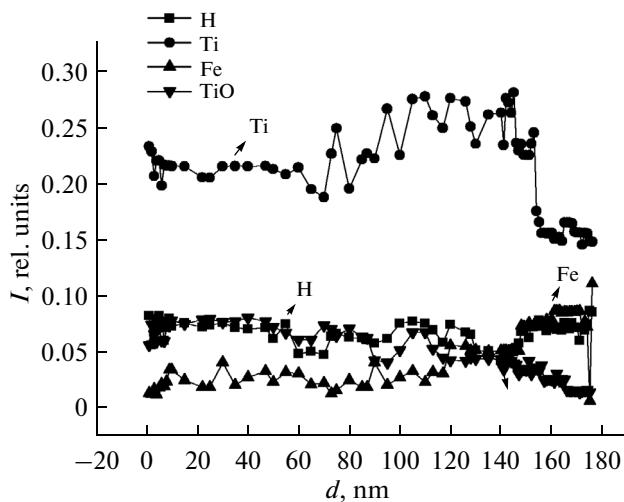


Fig. 2. Distribution of the yield of secondary ions of the main elements during sputtering of film no. 1₂ TiON.

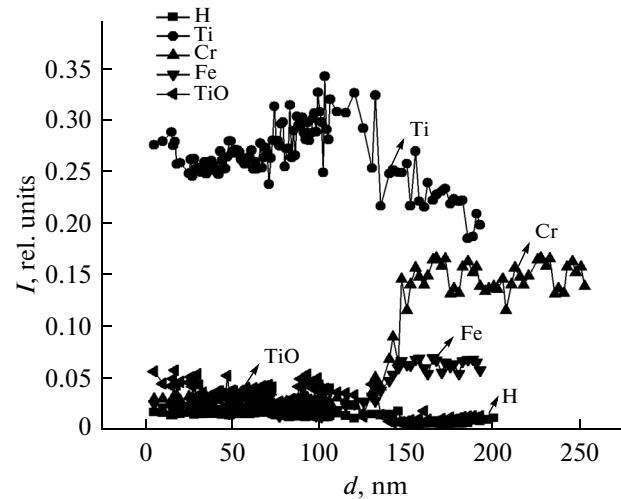


Fig. 3. Distribution of the yield of secondary ions of the main elements during sputtering of the film saturated with hydrogen no. 1₂ TiON.

in separate regions of the surface, and is revealed in the spectrum in the form of lines due to the bonds of TiN within the range 300–600 cm^{-1} and peaks NO_2 (or NO_3) of different intensities within the range 700–1700 cm^{-1} corresponding to different forms of nitrogen dioxide [10].

Experimental and basic studies made it possible to select the series of physical-chemical characteristics of the materials critical for biocompatibility with blood [6]. The property of wettability of the surface should be selected in this series. Strongly hydrophobic surfaces absorb more protein from blood plasma and induce significant structural changes in adsorbed proteins [6]. At the same time, the ability of hydrophilic coatings to prevent the deposition of proteins can become an obstacle against cellular colonization. An interrelation was also established between the level of hemocompatibility and the surface energy of the coating. There is a hypothesis of complementarity stating that hemocompatible materials during contact with blood should have the minimum value of the interphase free energy and the same character of distribution of the polar and dispersion components of the free energy of the surface of the material [6]. In this case the adsorption of the protein by the surface is minimized which increases its hemocompatibility. Thus, there is some uncertainty in the combination of physical-chemical characteristics of the surface determining its properties.

The main results of measuring the characteristics of coatings are given in Table 2. The obtained data show high values of the nanohardness and Young's modulus of the coatings indicating their high mechanical strength. The thickness of coatings formed in the bias mode is 27–30% less than the thickness of coatings formed in the mode of the grounded substrate. These results are conditioned by the fact that negative bias increases the flow of ions to the substrate and increases

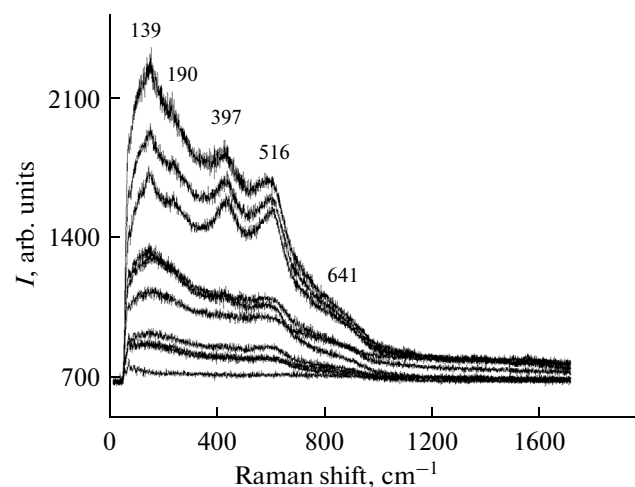


Fig. 4. Raman spectra of the sample no. 1₂ TiON.

the sputtering rate of the growing coating. The nanohardness of the coatings also depends on the evaporation mode. The nanohardness of coatings deposited in the bias mode is 10–48% higher than that deposited in the mode of the grounded substrate. This is associated with crystallization of the coating grains during their growth in the bias mode. The nanohardness value is 3.8–6.0 GPa, Young's modulus is 78–60 GPa regardless of the coating deposition mode. The number of works devoted to studying the mechanical characteristics of titanium oxynitride deposited by the method of reactive magnetron sputtering is very limited. Coatings deposited under different conditions have different mechanical characteristics. The results obtained in this work are in good agreement with the data of [2, 7], where the mechanical characteristics of oxynitride

Table 2. Characteristics of Ti-O-N coatings: L is the coating thickness, $\langle H \rangle$ is the nanohardness, $\langle E \rangle$ is Young's modulus, R_a is the roughness, θ_w is the contact angle of wetting with water, σ is the surface energy, σ_D is the dispersion component of the surface energy, σ_P is the polar component of the surface energy

Parameters	Substrate	Grounded substrate		Bias mode (–100 V)	
		no. 1, Ti–O–N	no. 3, Ti–O–N	no. 1 ₂ , Ti–O–N	no. 3 ₂ , Ti–O–N
sample	12Kh18N10T				
L , nm	–	270 ± 6	290 ± 7	190 ± 7	213 ± 8
R_a , nm	32 ± 2	35 ± 2	36 ± 2	25 ± 1	38 ± 2
$\langle H \rangle$, GPa	2 ± 0.2	4.3 ± 0.2	3.8 ± 0.2	4.7 ± 0.2	5.8 ± 0.2
$\langle E \rangle$, GPa	220 ± 8	67 ± 3	78 ± 5	65 ± 3	56 ± 4
θ_w , degrees	74 ± 2	106 ± 1	112 ± 2	94.5 ± 0.5	95 ± 3
σ , mJ/m ²	30 ± 2	9.9 ± 0.9	20 ± 4	15.6 ± 0.8	15 ± 2
σ_D , mJ/m ²	12 ± 1	4.5 ± 0.6	20 ± 4	6.1 ± 0.4	6.6 ± 0.9
σ_P , mJ/m ²	18 ± 1	5.4 ± 0.4	0.1 ± 0.1	9.5 ± 0.4	8.8 ± 0.8

coatings grown by the method of reactive magnetron sputtering were studied.

The obtained coatings are hydrophobic, the contact angle is larger than 90° for all evaporation modes. The maximum contact angle θ_w is 112° for sample no. 3, i.e., the coating deposited on the grounded substrate. The minimum contact angle θ_w is 94.5° , which corresponds to coating no. 1 Ti–O–N. Coatings grown in the bias mode are less hydrophobic than those grown on the grounded substrate.

The equal distribution of polar and dispersion components of the surface energy is characteristic for coatings grown in the bias mode. They correspond to the hypothesis of complementarity to the highest degree [6].

CONCLUSIONS

Films of titanium oxynitrides were prepared by the method of reactive magnetron sputtering. The structure of coatings has nanocrystal character with typical columnar microstructure in the case of a high oxygen concentration in the reactive gas. Anatase is dominant in the composition of the crystal phase of the coating. The obtained coatings have high values of nanohardness and Young's modulus which indicates their high mechanical strength. The coatings are hydrophobic and the contact angle has a value higher than 90° for all evaporation modes.

ACKNOWLEDGMENTS

This study was supported in part by the Government program "Science," research project no. 1524.

REFERENCES

1. A. Trenczek-Zajac, M. Radeckaa, and K. Zakrzewskab, *J. Power Sources*, No. 194, 93 (2009).
2. A. J. Aronson, D. Chen, and W. H. Class, *Thin Solid Films* **72**, 535 (1980).
3. E. N. Kudryavtseva, V. F. Pichugin, N. N. Nikitenkov, et al., *J. Surf. Invest.: X-ray, Synchrotron Neutron Tech.* **6**, 688 (2012).
4. M. E. Konishchev, O. S. Kuz'min, N. S. Morozova, and V. F. Pichugin, *Izv. Vyssh. Uchebn. Zaved., Fiz.* **55**, 235 (2012).
5. Yu. M. Shul'ga, D. V. Matyushenko, A. A. Golyshev, et al., *Tech. Phys. Lett.* **36**, 841 (2010).
6. V. I. Sevast'yanov and M. P. Kirpichnikov, *Biocompatible Materials* (Med. Inform. Agentstvo, Moscow, 2011) [in Russian].
7. M. Chandra Sekhara, P. Kondaiaha, S. V. Jagadeesh Chandraa, G. Mohan Raob, and S. Uthannaa, *Appl. Surf. Sci.* **258** (1789), 96 (2011).
8. A. N. Zeidel, *Principles of Spectral Analysis* (Nauka, Moscow, 1965) [in Russian].
9. V. Swamy, A. Kuznetsov, L. S. Dudrovinsky, R. A. Caryso, and B. C. Muddle, *Phys. Rev. B* **71**, 184 (2005).
10. N. Sergent, M. Epifani, and T. Pagnier, *Adv. Function. Mater.* **16**, 1488 (2006).
12. V. Swamy, A. Kuznetsov, L. S. Dudrovinsky, R. A. Caryso, and B. C. Muddle, *Phys. Rev. B* **71**, 184 (2005).

Translated by L. Mosina